Experimental Investigation of the Characteristics of Solid-Propellant, Velocity-Coupled Response Functions

L. L. Narayanaswami,* B. T. Zinn,† and B. R. Daniel‡
Georgia Institute of Technology, Atlanta, Georgia

This paper describes an experimental investigation of the validity of state-of-the-art approaches that use the so-called velocity-coupled response functions to determine the stability of solid-propellant rocket motors. These approaches are based upon the fundamental assumption that the propellant velocity-coupled response function is a propellant property independent of its location within the combustor. The applicability of this assumption was investigated in a modified impedance tube setup specifically developed for this study. It consisted of a "driver" propellant sample at the upstream end of the tube and "test" propellant samples on the side walls at a desired location downstream of the "driver" propellant. An acoustic driver located at the downstream end of the tube was used to simulate the flow conditions in an unstable rocket motor by exciting a standing acoustic wave of desired properties in the tube. The objective of the experiment was to measure the velocity-coupled response function of the "test" propellant samples. Tests were conducted with the "test" propellant samples at different locations along the impedance tube standing wave. The results clearly showed that the velocity-coupled response function is strongly dependent upon the propellant sample location relative to the impedance tube standing wave and thus cannot be considered a propellant property. The paper points out the need for a re-evaluation of current approaches for predicting the stability of solid-propellant rocket motors.

Nomenclature

a = speed of sound, m/s (ft/s)
A = cross-sectional area, m^2 (ft^2)
b = perimeter of the sidewall propellant samples, m (ft)
C_v = specific heat at constant volume J/kg · K (Btu/slug · °R)
G = gas phase bulk loss coefficient, N · s/m^4 (lb · s/ft^4)
Im( ) = imaginary part of ( )
k = constant in Eq. (1)
m = mass burn rate per unit area, kg/m^2 · s (slug/ft^2 · s)
p = pressure, Pa (lb/ft^2)
R = specific gas constant, J/kg · K (Btu/slug · °R)
R_p = pressure-coupled response function, nondimensional
R_v = velocity-coupled response function, nondimensional
t = time, s
T = temperature, K (°R)
u = velocity, m/s (ft/s)
u_t = threshold velocity, m/s (ft/s)
x = distance, m (ft)
γ = ratio of specific heats
ρ = density, kg/m^3 (slug/ft^3)
θ_p, θ_v = quantities defined in Eqs. (7) and (8)
ω = frequency, rad/s

Subscripts
b = properties at the sidewall propellant surface
F = flame property
0 = nonerosive conditions

Superscripts
$( )'$ = fluctuating quantity
$\bar{( )}$ = mean quantity

Introduction

THIS paper describes the application of the impedance tube technique in the investigation of the validity of current practices using the velocity-coupled response function to determine the stability of solid-propellant rocket motors.[1] Combustion instabilities occur when energy supplied by the combustion process excites one or more of the natural acoustic modes of the combustor. This driving by the solid-propellant combustion process depends upon the characteristics of space-dependent flow oscillations in the vicinity of the propellant surface. For example, in a rocket motor experiencing an instability of its fundamental, longitudinal acoustic mode, the propellant sections at the two ends of the motor experience primarily pressure oscillations, the propellant section at the center of the motor experiences primarily velocity oscillations parallel to its surface, and the remainder of the propellant grain experiences both velocity and pressure oscillations of varying amplitude and phase relationships. To determine the contribution of the entire propellant grain to the instability, the driving or damping provided by various sections of the propellant must be known. To date, this requirement has been interpreted as the need to know the propellant burn rate response to both pressure and velocity oscillations. These responses are generally referred to as the pressure- and velocity-coupled responses, respectively, and they are related to the pressure and velocity fluctuations through constant proportionality factors called the pressure- and velocity-coupled response functions.[1-3] While the existence of a pressure-coupled response function has been recognized for some time and has been the subject of a considerable number of investigations,[4-6] the higher complexity of the physicochemical processes affect-

Presented as Paper 85-0235 at the AIAA 23rd Aerospace Sciences Meeting Reno, NV, Jan. 14-17, 1985; received March 4, 1986; revision received Aug. 25, 1986. Copyright © American Institute of Aeronautics and Astronautics, Inc., 1987. All rights reserved.

*Postdoctoral Fellow, School of Aerospace Engineering; presently Assistant Professor, Embry-Riddle Aeronautical University, Daytona Beach, FL.
†Regents' Professor, School of Aerospace Engineering.
‡Senior Research Engineer, School of Aerospace Engineering.

ing the characteristics of the velocity-coupled response function has limited the number of investigations into its fundamental properties and applicability.

Before discussing existing velocity-coupled response models, it is instructive to briefly describe the current steady burn rate models. It is well known that the steady burning rate of a solid propellant depends upon the properties of the flow next to its surface, which under certain conditions cause erosive burning.[7,8] Developing the predictive capabilities of the steady burn rate and the associated erosive burning of solid propellants requires detailed analysis of the complex, multidimensional mixing, heat-transfer, and chemical processes that occur next to the propellant surface. While such approaches have been pursued by several investigators,[9-12] who have provided much insight into the causes of erosive burning, the complexity of the problem has, thus far, prevented the development of rigorous erosive burning models. In their absence, empirical models of erosive burning have been used to predict the performance of solid-propellant rocket motors. Experimental investigations of steady propellant burning indicate that there exists a threshold velocity u_t below which the burn rate is unaffected by the parallel flow[13-15] and above which the propellant burn rate is given by[16]

$$\bar{m}_b/m_{b0} = 1 + k(\bar{u} - u_t) \tag{1}$$

where k and u_t are determined experimentally. While models of this type are useful in design, they do not provide insight into the processes controlling this phenomenon.

By now, there is ample evidence that solid-propellant combustion processes are sensitive to the presence of velocity oscillations parallel to the propellant surface.[17-20] This sensitivity, which can be considered as the unsteady analog of steady-state erosive burning, is termed velocity coupling and the resulting burn rate oscillation is the velocity-coupled response. Considering the physics of the problem, one would expect that an oscillatory flow would produce oscillatory mixing, heat-transfer, and chemical processes next to the propellant surface which would result in an oscillatory propellant burn rate. When the proper phase relationship between the oscillatory propellant burn rate and the local pressure oscillations is established, a driving of the flow oscillations occurs. Consequently, it is of utmost importance to develop dependable analytical capabilities that can predict such propellant combustion/flow interactions. Again, as in the steady-state case, the complexity of the problem has prevented the development of reliable solid-propellant response models based upon fundamental principles and, consequently, all existing response models are heuristic in nature and are merely extensions of the empirical steady-state erosion model [see Eq. (1)] and concepts developed in pressure-coupling studies.

In modeling the velocity-coupled response it was argued 1) that the combustion process is responsive to only the magnitude of the flow velocity and is independent of the flow direction[17,21,22] and 2) that, when the magnitude of the total velocity (i.e., the vector sum of the steady and fluctuating velocities) is greater than the threshold velocity, the propellant response is proportional to the difference. Thus, the mass flux fluctuation due to a velocity oscillation parallel to the propellant surface is given by the relationship

$$\frac{m_b'}{\bar{m}_b} = \frac{R_v}{\bar{a}}\left[(|\bar{u} + u'| - u_t) - (\bar{u} - u_t)\right]$$

$$|\bar{u} + u'| > u_t,\ \bar{u} > u_t \tag{2}$$

where R_v is the velocity-coupled response function. Implicit in Eq. (2) is the assumption that R_v is a propellant property and thus independent of the propellant location within the combustor. While the validity of Eq. (2) has never been verified experimentally or theoretically, it has nevertheless served as a basis for a number of experimental investigations concerned with the determination of R_v as a propellant property.[2,3,25-27]

The manner in which a given propellant section responds to flow oscillations depends upon the structure of the steady-state combustion zone next to its surface, as different steady-state combustion zones may respond differently to oscillatory excitation. Since the local steady-state combustion zone is expected to depend upon the characteristics of the steady flow, it follows from the above discussion that both the steady and oscillatory components of the flow next to the propellant surface should affect the propellant response. Since the flow conditions within a rocket combustor are space dependent, the effect of the flow upon the propellant response is likely to be different at different combustor locations. Consequently, one would expect that the velocity-coupled response function R_v [see Eq. (2)], which is supposed to account for steady and unsteady flow and combustion effects, will also be space dependent.[28] This conjecture contradicts the underlying assumption of Eq. (2) that R_v is strictly a propellant property. Since the clarification of this contradiction is of crucial importance in the development of analytical capabilities for predicting the stability of solid-propellant rocket motors, both critical experimental and theoretical studies aimed at the resolution of this problem must be performed. This paper describes the results of an experimental investigation in which the impedance tube technique was used to explore this issue.

In what follows, a modified impedance tube technique, specifically developed for this study, is briefly discussed. This is followed by a description of the application of the technique in the investigation of the velocity-coupled responses of solid propellants. The paper closes with a discussion of the measured data and their implications for solid-propellant rocket motors stability analyses.

Modified Impedance Tube Technique

This section describes the measurement technique developed for this study. The impedance tube technique was initially developed by acousticians who utilized it to measure the sound-absorbing characteristics of various materials.[29,30] In these applications, the impedance tube consisted of a rigid-walled tube with the tested material placed across one end and an acoustic driver at the other. During a test, the driver was used to generate a train of acoustic waves of a desired frequency that propagated toward the tested material. These waves reflected off the tested sample with modified amplitude and phase and then combined with the incident wave train to form a standing wave in the tube. A traversing microphone was used to measure the structure of the resulting standing wave and these data together with appropriate analytical solutions were utilized to determine the amplitude and phase changes occurring at the tested sample surface—data that determined the sound-absorbing characteristics of the tested material. Subsequently, this technique was modified to determine the admittances of choked nozzles,[31] acoustic liners,[32] and pressure-coupled responses of burning solid propellants.[33,34] In this investigation, the impedance tube technique was further modified to investigate the velocity-coupled responses of solid propellants.

A schematic of the modified impedance tube setup used in this study is shown in Fig. 1. The objective of the experiment is to measure the velocity-coupled response function of the "test" propellant samples. The "driver" propellant sample provides a stream of hot combustion products that flows past the "test" propellant samples in an attempt to simulate actual rocket motor flow conditions. In this configuration, the "driver" propellant experiences only pressure oscillations, while the "test" propellant samples are subjected to both pressure and velocity oscillations. The experimental setup permits moving the "driver" propellant to different locations upstream of the "test" samples, a capability that enables the investigation of the response of the "test" propellant samples at different acoustical environments along the standing wave.

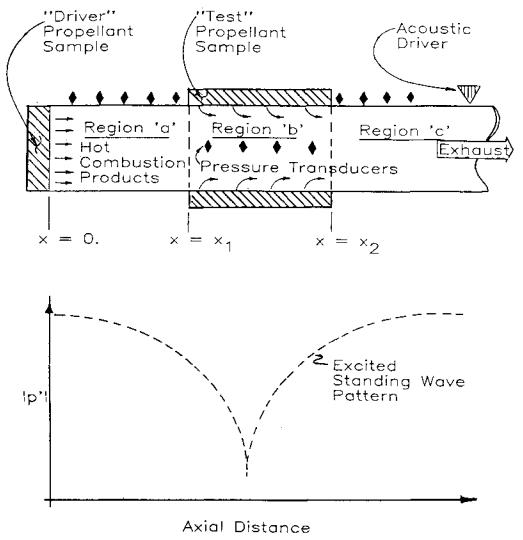

Fig. 1 Schematic of the velocity-coupled impedance tube.

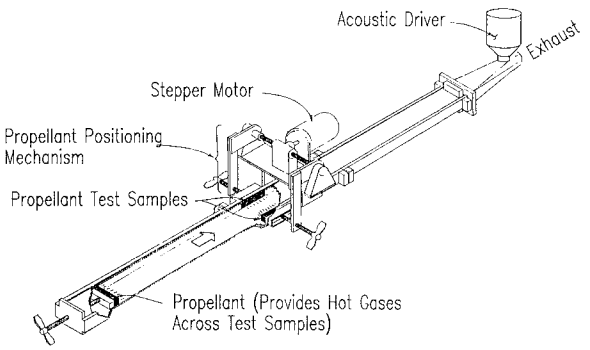

Fig. 2 Modified impedance tube for velocity-coupling measurements.

In an experiment to determine the velocity-coupled response function, the acoustic driver is first used to set up a standing wave of a desired frequency in the impedance tube. Next, the propellant samples are ignited and a series of transducers mounted at preselected locations along the impedance tube walls is used to measure the continuously varying (due to the presence of propellant ignition, quasisteady state burning, and extinguishment periods) wave structure in the impedance tube. These pressure transducers are used in this setup because the short duration (1–3 s) of a test precludes the use of a traversing microphone for measuring the wave structure. While the test is in progress, a stepping motor is utilized to keep the "test" propellant surfaces flush with the adjacent impedance tube walls. The measured acoustic pressure data are used to determine the unknown velocity-coupled response function by utilizing a data reduction procedure specifically developed for this purpose.

The issues raised in the previous section were investigated in this study by measuring the value of R_v in tests in which the "test" propellant samples were placed at different locations along the standing wave structure. Finding that the same (or close) values for the response function R_v were obtained in all of these tests would support the argument that R_v is a propellant property independent of location—and vice versa.

Theoretical Considerations

These theoretical studies were undertaken with the objective of developing an analytical methodology for determining the velocity-coupled response function from measured impedance tube pressure data. The system of conservation equations used to determine the axial and linear stability limits of solid-propellant rocket motors also serves as the starting point for this study. It consists of the linearized, one-dimensional mass, momentum, and energy conservation equations. Neglecting terms of $\mathcal{O}(\bar{u}^2)$ and assuming a periodic time dependence of the solutions, these wave equations can be expressed as follows.[34,35]

Continuity:

$$i\omega\rho' + \frac{\mathrm{d}}{\mathrm{d}x}(\bar{\rho}u' + \bar{u}\rho') = \frac{b}{A}m_b' \tag{3}$$

Momentum:

$$i\omega\bar{\rho}u' + \bar{\rho}\bar{u}\frac{\mathrm{d}u'}{\mathrm{d}x} + \bar{\rho}\frac{\mathrm{d}\bar{u}}{\mathrm{d}x}u' + \frac{\mathrm{d}p'}{\mathrm{d}x} + \frac{b}{A}\bar{m}_b u' + Gu' = 0 \tag{4}$$

Energy:

$$i\omega p' + \bar{u}\frac{\mathrm{d}p'}{\mathrm{d}x} + \gamma\bar{p}\frac{\mathrm{d}u'}{\mathrm{d}x} + \gamma\frac{\mathrm{d}\bar{u}}{\mathrm{d}x}p' = \frac{b}{A}\bar{m}_b\bar{E}\left(\frac{m_b'}{\bar{m}_b} + \frac{E'}{\bar{E}}\right) \tag{5}$$

where $\bar{E}$ and E' are, respectively, the steady and perturbation components of

$$E = \gamma RT_F + (R/2C_v)(u^2 + u_b^2) \tag{6}$$

which describes the energy addition at the propellant surface.

Examination of the above equations shows that the momentum and energy equations are decoupled from the continuity equation, since they contain only the dependent variables p' and u'. These equations can be solved, provided the expression

$$\frac{b}{A}\bar{m}_b\bar{E}\left(\frac{m_b'}{\bar{m}_b} + \frac{E'}{\bar{E}}\right)$$

on the right-hand side of the energy equation is known. This expression describes the response of the propellant to the pressure and velocity oscillations in the flowfield. To date, it has been customary[1,3,6] to express the pressure-coupled response in the following form:

$$\left(\frac{m_b'}{\bar{m}_b} + \frac{E'}{\bar{E}}\right)_{p'} = (R_p + \theta_p)\frac{p'}{\bar{p}} \tag{7}$$

where R_p is the pressure-coupled response function and θ_p relates $E'/\bar{E}$ to p'. Assuming that the threshold velocity u_t is zero and that the mean velocity is greater than the acoustic velocity (i.e., $\bar{u} > |u'|$), the velocity-coupled response can be obtained from Eq. (2) as

$$\left(\frac{m_b'}{\bar{m}_b} + \frac{E'}{\bar{E}}\right)_{u'} = (R_v + \theta_v)\frac{u'}{\bar{a}} \tag{8}$$

where R_v is the velocity-coupled response function and θ_v relates $E'/\bar{E}$ to u'. Finally, assuming that the propellant responses to the pressure and velocity oscillations are additive, the total propellant response can be expressed as

$$\frac{m_b'}{\bar{m}_b} + \frac{E'}{\bar{E}} = (R_p + \theta_p)\frac{p'}{\bar{p}} + (R_v + \theta_v)\frac{u'}{\bar{a}} \tag{9}$$

It is important to note that the driving of oscillations in a combustor by velocity coupling will occur only if the velocity-coupled response has a component in phase with the local

pressure oscillation. Since the acoustic velocity oscillation u' is 90 deg out of phase with the local pressure oscillation, it is clear from Eq. (8) that velocity-coupled driving will occur only if the response function $(R_v + \theta_v)$ introduces a 90 deg phase change that results in the propellant velocity-coupled response having a component in phase with the local pressure oscillation. Consequently, it is the imaginary part of the velocity-coupled response function that determines the contribution of velocity coupling to rocket motor stability.[24]

When $(R_p + \theta_p)$ and $(R_v + \theta_v)$ are known, Eqs. (3–9) can be used to predict the characteristics of the standing wave inside the impedance tube or the stability of a solid-propellant rocket motor. Alternately, these equations provide a starting point for the determination of $(R_v + \theta_v)$ from measured impedance tube data. To optimize the planned impedance tube experiments, Eqs. (3–9) were used in a parametric study[35,36] that investigated whether changes in the velocity-coupled response function $(R_v + \theta_v)$ produced measurable changes in the impedance tube wave structure. This study revealed that the largest changes in the impedance tube wave structure, due to changes in $(R_v + \theta_v)$, occured in the vicinity of the acoustic pressure minima. Consequently, accurate measurements of the wave structure near these minima are required to accurately determine $(R_v + \theta_v)$.

The next step is the development of a suitable data reduction procedure to determine the velocity-coupled response function from the measured acoustic pressure data. The developed data reduction procedure is based on the method of quasilinearization and it determines $(R_v + \theta_v)$ by minimizing the error function E_Φ given by

$$E_\Phi = \sum_N [\Phi_m(x_i) - \Phi_c(x_i)]^2 \qquad (10)$$

by requiring that

$$\frac{\partial E_\Phi}{\partial [Re(R_v + \theta_v)]} = \frac{\partial E_\Phi}{\partial [\mathrm{Im}(R_v + \theta_v)]} = 0 \qquad (11)$$

where $\Phi_m(x_i)$ and $\Phi_c(x_i)$ are measured and computed [i.e., solution of Eqs. (3–5)] values of the phase angles at N different locations in the impedance tube. For details, the reader is referred to Ref. 35. It should be noted, however, that the developed data reduction procedure presumes knowledge of the pressure-coupled response function. Consequently, the pressure-coupled response function has to be determined in a separate experiment or by the use of a reliable theory.

Experimental Efforts

The modified impedance tube developed for the investigation of the velocity-coupled response of solid propellants is shown in Fig. 2. It is approximately 6 ft (1.83 m) long with a 4×1 in. (0.1×0.025 m) rectangular cross section and it has provisions for mounting 4 in. (0.1 m) long "test" propellant samples on the sidewalls. Special adaptors for holding the Sundstrand pressure transducers (model 211B-5) used in this study are available at 0.3 in. (0.75 cm) intervals along the upper wall. An electropneumatic Ling EPT-94B acoustic driver is mounted a short distance upstream of the exhaust end and a spectral dynamic oscillator (model SD104A-5) is used to control the frequency and amplitude of the oscillations generated by the driver. During an experiment, the entire setup is placed inside a high-pressure tank to simulate actual rocket motor conditions.

The data acquisition system (Fig. 3) consisted of a HP2100S minicomputer equipped with a HP7901A disk drive and a Preston analog-to-digital converter. The system acquired 30,000 samples/s/channel and could handle up to 16 channels of data simultaneously. The analog data from all the transducers were digitized and stored for post-test analysis by this system.

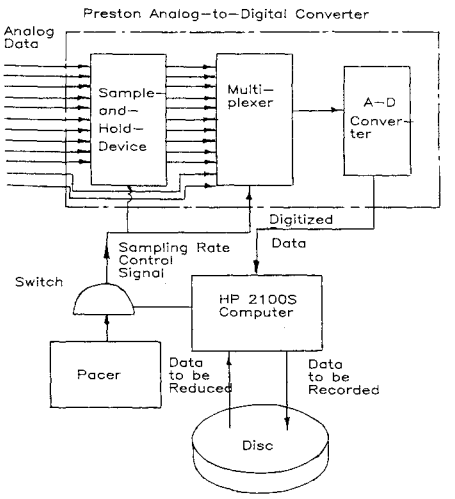

Fig. 3 Data acquisition system.

All the velocity-coupled response function measurements were conducted at a pressure of 300 psig (2.067×10^6 Pa gage). With the tank pressurized and a standing wave of a desired frequency established in the impedance tube, the propellant samples were ignited and a test initiated. The test duration was divided into a series of data acquisition periods, separated from each other by periods of data transfer. During the data acquisition periods, called blocks, the analog data from all of the channels (that is, transducers) were digitized and stored in the computer memory. Each block could be programmed to acquire data over a time period whose duration was an integer multiple of 12 periods of the driven oscillation. During the data transfer periods, the digitized data were transferred from the computer memory onto the disk to make room in the memory for data from the next block. Thus, data were collected over discrete periods of time (i.e., blocks) as no data were acquired during data transfer periods. After the test, the stored data in each block were numerically Fourier-analyzed to obtain the amplitudes and phases of the measured data at the test frequency. Typical time histories of the amplitude and phase of the measured data obtained at one transducer location are shown in Fig. 4. Examination of this figure shows the existence of ignition and extinguishment transients with a quasisteady period in between. Such time histories were obtained for all channels of data. Using these time histories, the spatial amplitude and phase distributions in the impedance tube could be obtained at any instant during the quasisteady period. These data were then input into the data reduction program to determine the desired propellant velocity-coupled response function.

Results and Discussion

Several velocity-coupled response function determination tests were performed; these tests differed from one another by the frequency of the oscillation and the location of the "test" propellant samples along the standing wave structure. The same nonaluminized propellant, designated UZ-7, was used in all of these experiments. The measured data from these tests are presented and discussed in this section.

As stated earlier, a reliable determination of the velocity-coupled response function requires a careful measurement of the standing wave structure in the vicinity of the acoustic pressure node. Therefore, many of the pressure measurements had to be performed near the pressure node where the desired signal was masked by noise from other sources, and signal averaging was required to reduce the effect of this noise. Since the available memory of the minicomputer limited the amount of data that could be recorded in a given block, an estimate of the minimum averaging time needed to sufficiently enhance

the signal-to-noise ratio was required. This problem was investigated by comparing data averaged over different numbers of cycles of the test signal. The spatial amplitude and phase distributions obtained by averaging data measured during the quasisteady burning period over 18, 36, and 72 cycles are compared in Figs. 5 and 6, respectively. Examination of these figures shows that the amplitude and phase data obtained as an "18 cycle average" exhibit considerable scatter about the "72 cycle average," while the "36 cycle average" data are consistent with the "72 cycle average" data. This indicates that averaging data over 36 cycles provides sufficient enhancement of the signal-to-noise ratio.

In the experiments to determine the velocity-coupled response functions, the spatial amplitude and phase distributions were obtained by averaging the measured signals over 36 cycles. The needed pressure-coupled response functions ($R_p + \theta_p$) were measured by the pressure-coupled impedance tube technique, the details of which can be found elsewhere.[34,35]

The initial velocity-coupled determination tests were conducted at a frequency of 600 Hz. In the first of these tests, the "test" samples were located upstream of the first pressure minimum and acoustic pressure data measured around this minimum were used to determine ($R_v + \theta_v$). In the second experiment, the "test" samples were located downstream of the first minimum and the acoustic pressure data measured around the second acoustic pressure minimum were used to determine ($R_v + \theta_v$). The standing wave structures measured in these experiments are shown in Figs. 7 and 8. Also shown in these figures are the determined wave structures that provided the "best" agreement with the experimental data. The determined, optimum values of $\mathrm{Im}(R_v + \theta_v)$ that provided the "best" agreement are also presented in the figures.

An examination of Figs. 7 and 8 shows that there is satisfactory agreement between the measured and computed wave structures. However, the value of $\mathrm{Im}(R_v + \theta_v)$ determined in the first experiment is considerably different from that obtained in the second; that is, the data indicate that $\mathrm{Im}(R_v + \theta_v)$ of the propellant sample upstream of the pressure minimum is -3 and that it equals 30 when the propellant sample is located downstream of the pressure minimum. Considerations of the physics of the problem together with the measured data indicate that in both tests the velocity-coupled responses of the tested propellant samples attenuated the oscillations in the impedance tube. Qualitative support for this argument was provided by the observation that in both tests the amplitudes of the oscillations in the impedance tube decreased after propellant samples ignition.

Considering their complexity, it was of utmost importance to check the repeatability of the velocity-coupled determination experiments. Figure 9 compares the time history of the acoustic-pressure phases measured in two different velocity-coupled tests. The frequency of the driven oscillations and the location of the "test" propellant samples were the same in both these tests. The similarity in the time histories and the excellent agreement between the determined values of $\mathrm{Im}(R_v + \theta_v)$ demonstrate the repeatability of the developed experimental technique.

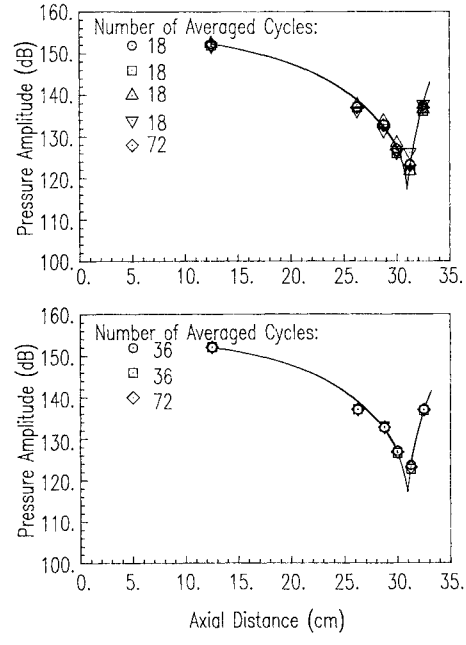

Fig. 5 Comparison of spatial amplitude distributions obtained by averaging the pressures measured during the quasisteady burning period over 18, 36, and 72 cycles.

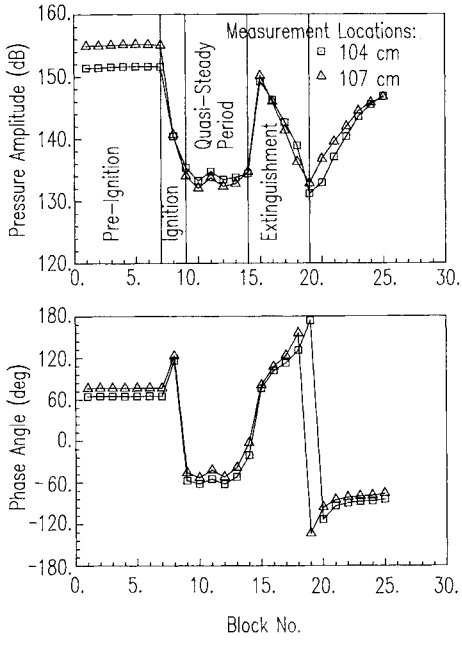

Fig. 4 Typical time variations of measured pressure amplitudes and phases at two tube locations (note the various test periods).

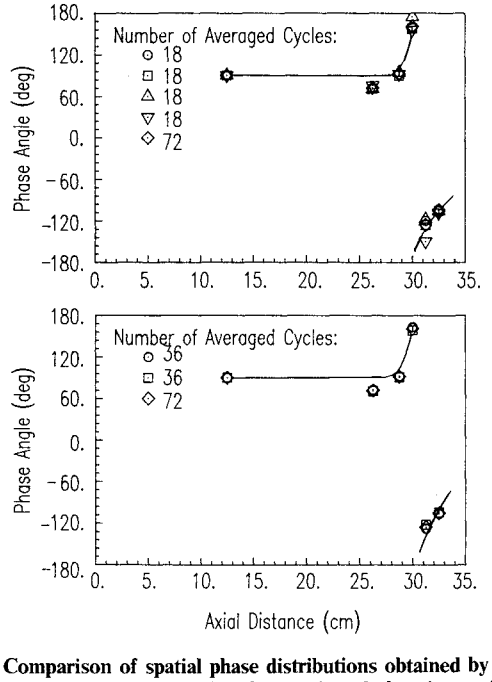

Fig. 6 Comparison of spatial phase distributions obtained by averaging the pressures measured during the quasisteady burning period over 18, 36, and 72 cycles.

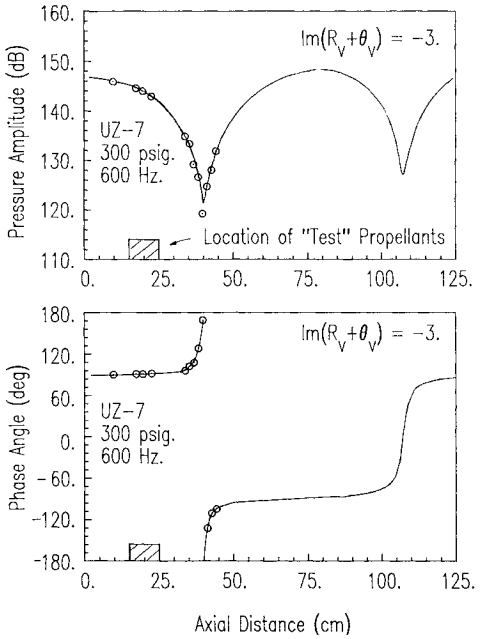

Fig. 7 Comparison of the experimentally and theoretically determined axial dependencies of the amplitude and phase of the impedance tube standing wave when the "test" samples were located upstream of the first pressure minimum.

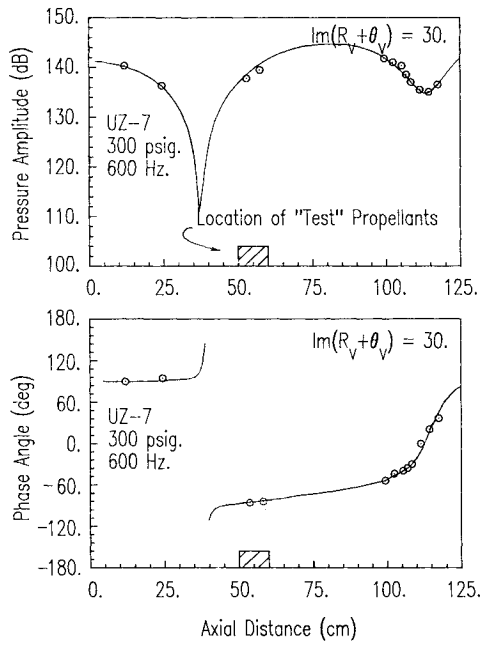

Fig. 8 Comparison of the experimentally and theoretically determined axial dependencies of the amplitude and phase of the impedance tube standing wave with the "test" samples located downstream of the first pressure minimum.

Velocity-coupled determination tests were also performed at 800 Hz with the "test" propellant samples located upstream of the first pressure minimum in one test and downstream of this minimum in another. The measured wave structures obtained in these tests are compared with the computed structures in Figs. 10 and 11. Again, the measured value of $\mathrm{Im}(R_v + \theta_v)$ of the propellant sample upstream of the pressure minimum was considerably different from the value measured downstream of the minimum. Furthermore, in both tests, the interactions between the "test" propellant samples combustion processes and the impedance tube oscillations resulted in wave attenuation.

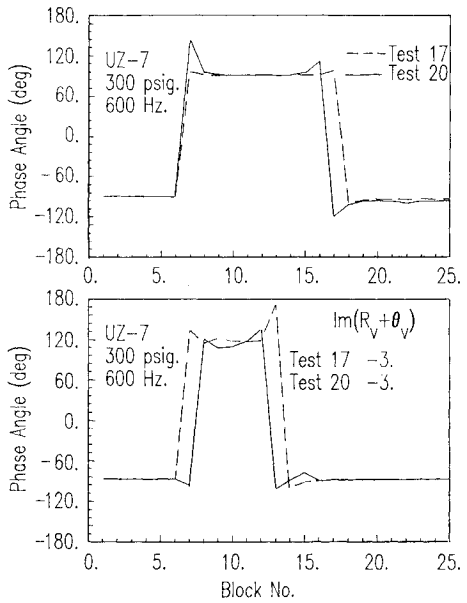

Fig. 9 Comparison of the phase data measured at two tube locations in two different velocity-coupled tests.

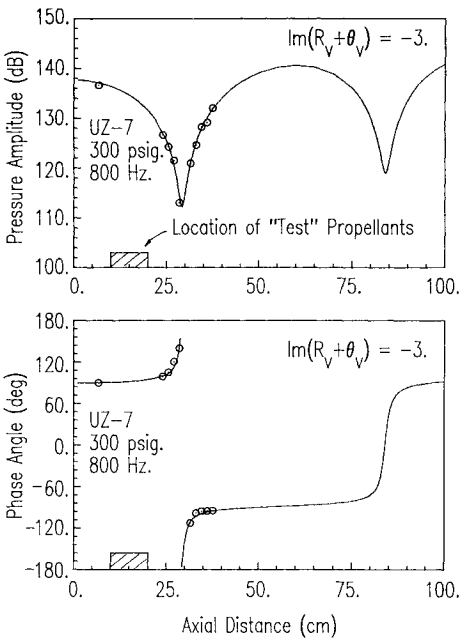

Fig. 10 Comparison of the experimental and theoretically determined axial variations of the amplitude and phase of the impedance tube standing wave when the "test" samples were located upstream of the first pressure minimum.

The above reported data clearly show that the same propellant samples possess different velocity-coupled response functions when positioned at different locations along a standing acoustic wave. Consequently, it must be concluded that the velocity-coupled response function cannot, in general, be regarded as a propellant property and that stability analyses based upon this notion are bound to yield erroneous rocket motor stability limits. While the results of this study clearly indicate that the propellant burn rate indeed responds to velocity oscillations parallel to the propellant surface, the nature of this response is currently not understood. Considering the importance of this type of response in solid-propellant rocket motors stability analyses, it is strongly recommended that new endeavors aimed at the understanding of this type of propellant response be undertaken.

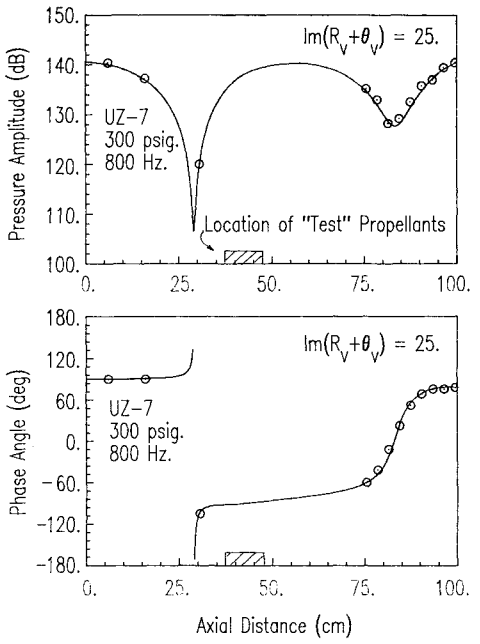

Fig. 11 Comparison of the experimental and theoretically determined axial variations of the amplitude and phase of the impedance tube standing wave with the "test" samples located downstream of the first pressure minimum.

The results reported herein also point out a misconception in current considerations of the contribution of velocity coupling to motor stability. It has been argued that velocity coupling does not contribute to the linear stability of the fundamental axial mode because the standing pressure wave undergoes a 180 deg phase change between the fore and aft ends of the rocket motor. Consequently, neglecting asymmetries introduced by mean flow effects, if the assumption that the velocity-coupled response function is independent of location in the rocket motor holds, one-half of the propellant will drive the oscillation and the remaining half will attenuate the oscillation with no net contribution to the driving of the combustor oscillation from velocity coupling. The results of this investigation indicate that the velocity-coupled response function varies with location in the combustor and, consequently, velocity coupling may contribute to the linear stability of the fundamental axial mode in a solid-propellant rocket motor, even if asymmetries introduced by mean flow effects are not important.

Acknowledgments

This research was sponsored by the U.S. Air Force Office of Scientific Research, Contract F 49620-82-C-0013.

References

[1]Culick, F.E.C., "Stability of Longitudinal Oscillations with Pressure and Velocity Coupling in a Solid Propellant Rocket," *Combustion Science and Technology*, Vol. 2, No. 4, Dec. 1970, pp. 179–201.

[2]Micci, M.M., Caveny, L.H., and Sirignano W.H., "Linear Analysis of Longitudinal Waves in Rocket Motor Chambers," *AIAA Journal*, Vol. 19, Feb. 1981, pp. 198–204.

[3]Brown, R.S., Waugh, W.C., and Kelly, V.L., "Rotating Valve for Velocity-Coupled Combustion Response Measurements," AIAA Paper 81-1522, 1982.

[4]Brown, R.S., Culick, F.E.C., and Zinn, B.T., "Experimental Methods for Combustion Admittance Measurements," *AIAA Progress in Astronautics and Aeronautics: Experimental Diagnostics in Combustion of Solids*: Vol. 63, edited by T.L. Boggs and B.T. Zinn, AIAA, New York, 1978, pp. 191–220.

[5]Culick, F.E.C., "T-Burner Testing of Metallized Solid Propellants," AFRPL-TR-74-28, Final Rept., 1974.

[6]Perry, E.H., "Investigation of the T-Burner and its Role in Combustion Instability Studies," Ph.D. Thesis, California Institute of Technology, Pasadena, 1970.

[7]Kuo, K.K. and Razdan, M.K., "Review of Erosive Burning of Solid Propellants," 12th JANNAF Combustion Meeting, CPIA Pub. 273, Vol. II, 1975, pp. 323–338.

[8]Marklund, T. and Lake, A., "Experimental Investigation of Propellant Erosion," *ARS Journal*, Vol. 3, No. 2, 1960, pp. 173–178.

[9]Corner, J., *Theory of Internal Ballistics of Guns*, Wiley, New York, 1950.

[10]Tsuji, H., "An Aerothermochemical Analysis of Erosive Burning of Solid Propellant," *Ninth (International) Symposium on Combustion*, The Combustion Institute, Pittsburgh, PA, 1963, pp. 384–393.

[11]Razdan, M.K., "Theoretical Studies of Erosive Burning of Double Base Solid Propellants," Master of Technology Thesis, Indian Institute of Technology, Kanpur, India, 1974.

[12]Razdan, M.K. and Kuo, K., "Erosive Burning Studies of Composite Propellants by the Reacting Turbulent Boundary-Layer Approach," AFOSR-76-2914, Final Rept., 1977.

[13]Kreidler, J.W., "Erosive Burning—New Experimental Techniques and Methods of Analysis," AIAA Paper 64-155, 1964.

[14]Zucrow, M.J., Osborn, J.R., and Murphy, J.M., "An Experimental Investigation of the Erosive Burning Characteristics of a Nonhomogeneous Solid," AIAA Paper 64-107, 1964.

[15]Wimpress, R.N., *Internal Ballistics of Solid Fuel Rockets*, McGraw-Hill, New York, p. 129, 1950.

[16]Heron, R., *Internal Ballistic Problems of Solid Propellant Rocket Technology*, Vol. 1, Plenum Press, New York, 1961.

[17]Hart, R.W., Bird, J.F., and McClure, F.T., "The Influence of Erosive Burning on Acoustic Instability in Solid Propellant Rocket Motors," *AIAA Progress in Astronautics and Rocketry: Solid Propellant Rocket Research*, Vol. 1, edited by M. Summerfield, Academic Press, New York, 1960, pp. 423–451.

[18]Bird, J.F., Hart, R.W., and McClure, F.T., "Finite Acoustic Oscillations and Erosive Burning in Solid Fuel Rockets," *AIAA Journal*, Vol. 3, Dec. 1965, pp. 2248–2256.

[19]Price, E.W. and Dehority, G.L., "Velocity Coupled Axial Mode Combustion Instability in Solid Propellant Rocket Motors," *ICRPG/AIAA Second Propulsion Conference*, 1967, pp. 213–217.

[20]Price, E.W., "Evidence for Velocity Coupling," Paper presented at First ICRPG Combustion Instability Conference, Orlando Air Force Base, FL, 1964.

[21]McClure, F.T., Hart, R.W., and Bird, J.F., "Solid Propellant Rocket Motors as Acoustic Oscillators," *AIAA Progress in Astronautics and Rocketry: Solid Propellant Rocket Research*, Vol. 1, edited by M. Summerfield, Academic Press, New York, 1960, pp. 295–358.

[22]McClure, F.T., Bird, J.F., and Hart, R.W., "Erosion Mechanism for Non-Linear Instability in the Axial Modes of Solid Propellant Rocket Motors," *ARS Journal*, Vol. 32, No. 3, March 1962, pp. 374–378.

[23]Micheli, P., "Investigation of Velocity Coupled Combustion Instability," AFRPL-TR-75-54, Interim Report, 1975.

[24]Culick, F.E.C., "Velocity Coupling Analysis," NWC TP 6363, 1983.

[25]Stepp, E.E., "Effect of Pressure and Velocity Coupling on Low Frequency Instability," *AIAA Journal*, Vol. 5, May 1967, pp. 945–948.

[26]Beckstead, M.W., Horton, M.D., Krashin, M., and Butcher, A.G., "Velocity Coupling Combustion Instability," AFRPL-TR, Final Rept., 1973.

[27]Kuentzmann, P. and Lengelle, G., "Recent Research Activity at ONERA on Combustion Instability and Erosive Burning," Paper presented at Joint AFOSR/AFRPL Rocket Propulsion Meeting, Lancaster, CA, 1977.

[28]Price, E.W., "Velocity-Coupling in Oscillatory Combustion of Solid Propellants," *AIAA Journal*, Vol. 17, July 1979, pp. 799–800.

[29]Scott, R.A., "An Apparatus for Accurate Measurement of the Acoustic Impedance of Sound Absorbing Materials," *Proceedings of the Physical Society*, Vol. 58, 1946, pp. 253–264.

[30]Lippert, W.K.R., "The Practical Representation of Standing Waves in an Acoustic Impedance Tube," *Acustica*, Vol. 3, No. 3, 1953, pp. 153–160.

[31] Bell, W.A., "Experimental Determination of Three Dimensional Liquid Rocket Nozzle Admittances," Ph.D. Thesis, School of Aerospace Engineering, Georgia Institute of Technology, Atlanta, 1972.

[32] Zinn, B.T., Daniel, B.R., Janardan, B.A., and Smith, A.J. Jr., "Damping of Axial Instabilities by Minuteman II, Stage III, Minuteman III, Stage III, Exhaust Nozzles," AFRPL-TR-72-71, Interim Report, 1972.

[33] Salikuddin, M., "Application of the Impedance Tube Technique in the Measurement of Burning Solid Propellant Admittances," Ph.D. Thesis, School of Aerospace Engineering, Georgia Institute of Technology, Atlanta, 1978.

[34] Baum, J.D., "Experimental Determination of the Admittances of Solid Propellants by the Impedance Tube Technique," Ph.D. Thesis, Georgia Institute of Technology, Atlanta, 1980.

[35] Narayanaswami, L.L., "Investigation of the Pressure- and Velocity-Coupled Responses of Solid Propellants Using the Impedance Tube Technique," Ph.D. Thesis, Georgia Institute of Technology, Atlanta, 1984.

[36] Zinn, B.T. and Narayanaswami, L., "Application of the Impedance Tube Technique in the Measurement of the Driving Provided by Solid Propellants During Combustion Instabilities," *Acta Astronautica*, Vol. 9, No. 5, 1982, pp. 303–315.

From the AIAA Progress in Astronautics and Aeronautics Series...

ENTRY HEATING AND THERMAL PROTECTION—v. 69

HEAT TRANSFER, THERMAL CONTROL, AND HEAT PIPES—v. 70

Edited by Walter B. Olstad, NASA Headquarters

The era of space exploration and utilization that we are witnessing today could not have become reality without a host of evolutionary and even revolutionary advances in many technical areas. Thermophysics is certainly no exception. In fact, the interdisciplinary field of thermophysics plays a significant role in the life cycle of all space missions from launch, through operation in the space environment, to entry into the atmosphere of Earth or one of Earth's planetary neighbors. Thermal control has been and remains a prime design concern for all spacecraft. Although many noteworthy advances in thermal control technology can be cited, such as advanced thermal coatings, louvered space radiators, low-temperature phase-change material packages, heat pipes and thermal diodes, and computational thermal analysis techniques, new and more challenging problems continue to arise. The prospects are for increased, not diminished, demands on the skill and ingenuity of the thermal control engineer and for continued advancement in those fundamental discipline areas upon which he relies. It is hoped that these volumes will be useful references for those working in these fields who may wish to bring themselves up-to-date in the applications to spacecraft and a guide and inspiration to those who, in the future, will be faced with new and, as yet, unknown design challenges.

Published in 1980, Volume 69—361 pp., 6 × 9, illus., $25.00 Mem., $45.00 List
Published in 1980, Volume 70—393 pp., 6 × 9, illus., $25.00 Mem., $45.00 List

TO ORDER WRITE: Publications Dept., AIAA, 1633 Broadway, New York, N.Y. 10019